



Coriolis

n°5, January 2009 - <http://www.ifremer.fr/coriolis/>

Editorial

MyOcean kicked off for a 3-year challenging period

Pierre Bahurel, MyOcean coordinator.

2009 has a special meaning for the MyOcean partners: it means entering into a 3-year challenging and intensive period where they have to implement and demonstrate the value of the European Marine Core Service, one of the top-three pillars of the European GMES program. This is undoubtedly one of the most important challenges of the coming years for the ocean monitoring and forecasting community.

MyOcean¹ is devoted to the implementation of the "European Marine Core Service": "European" means that the MyOcean definition is driven by the search of a real pan-European added-value (ie identify and implement what could be done better or only done thanks to a pan-European framework) ; "Marine Core" means that the information provided by MyOcean is focussed on a generic information on the ocean, commonly used as the "core" input to a wide range of different applications (ie monitor and forecast currents, temperature, salinity, ice extent, primary biogeochemical variables... without developing here user specific information); and "Service" means that MyOcean is devoted to service to users, and that the scientific and technical effort is driven by their requirements (ie find the relevant balance between a scientific-push and a user-pull situation).

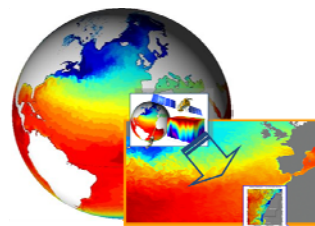
Shortly speaking, MyOcean has to set up and run a new and integrated capacity in Europe to provide on an operational basis to anyone requesting it high-quality reference generic information on the state of the oceans, composed of space observations, in situ observations and assimilative model outputs, covering the global ocean and European regional seas, depicting the past 25 years, the real-time situation and short-term forecast.

The MERSEA FP6 project (2004-2008) built a pan-European approach on the integration of the different existing ocean monitoring and forecasting facilities; its success paved the way to MyOcean (2009-2011) devoted to the transition to an operational service. The 2-year negotiation between the European Commission (co-funding this FP7 project) and the MyOcean consortium (composed of 60 partners around Europe) has been positively ended at the end of 2008: objectives, plan and organization are precisely set and agreed. On the 1st of January 2009, MyOcean turned into the active preparation of teams and implementation plan for the official kick-off set to the 1st of April. Here we are with this challenging period.



¹ see also a description of MyOcean in "Coriolis and Europe: the way forward" by S. Pouliquen and P.-Y. Le Traon, issue n°4 of this newsletter, September 2007.

Coriolis has a key role to play in MyOcean: it's the MyOcean reference centre for in situ. The MyOcean monitoring and forecasting facility is based on 12 key production components: 5 of them are dealing with observations (the Thematic Assembly Centres - TACs) and 7 are dealing with assimilative models (the Monitoring and Forecasting Centres - MFCs). Coriolis is leading the In Situ TAC which is the MyOcean reference centre for any data and information based on in situ observations: a reference centre for any of the 60 partners of the consortium, representing 28 different nations throughout Europe and associate countries; and a reference centre for any user of the MyOcean service, requiring more information on the in situ information. The MyOcean In Situ TAC has adopted a pan-European organization with a coordination role and global ocean mission set to the Coriolis centre in Brest, and regional specificities handled thanks to six regional centres throughout Europe to cover the Arctic, the Baltic, the Atlantic North-West Shelves, the Atlantic Irish-Biscay-Iberic, the Mediterranean and the Black Sea areas.



In this Issue

Editorial:

MyOcean kicked off for a 3-year challenging period.....p 1

DataCenter:

Processing and Quality Checks of Shipboard ADCP Data.....p 2

Progress in Argo Delayed Mode Quality Controlp 3

In-Situ Delayed Mode at Coriolis Data Center: 1990-2007 Reference datasetp 5

Instrumentation:

First Success of ProvBio floats.....p 6

Coriolis Science & GMMC:

A scientific team for the Coriolis Projectp 8

SSS-fronts properties deduced from TSG data in the North Atlantic Subpolar Gyrep 10

When satellite altimetry is called for to help on Argo quality control issues.....p 13

Vertical variability of Near-Surface Salinity in the Tropics: Consequences for SMOS Calibration and Validation ...p 15

Barrier Layer Variability in the Western Pacific Warm Pool, as inferred from Argo floats during 2000-2007p 15

Beyond the unceasing quest for better observations, in quantity and quality, demanding long-term science and technical investments, MyOcean means at least three challenges for the in situ community:

- implement and *demonstrate the capacity of a real operational service* in Europe for qualified in situ data handling and dissemination, able to manage multiple sources of data and a multi-centre organization distributed on the European territory, with the quality and the reliability requested from operational organizations,

- develop and *promote the added-value of in situ information* in the European Marine Core Service reference core products, by providing high-value inputs to the final synthetic products based on data combination and data assimilation into models,
- in parallel to the MyOcean service implementation, contribute and organize *support to the in situ observation network* sustainability in the European GMES framework, and build joint strategies in Europe for the sustainability of the marine space and in situ observation networks and the MyOcean marine monitoring and forecasting service.

Processing and Quality Checks of Shipboard ADCP Data

Vanessa Tosello, Nolwenn Carn, Michèle Fichaut, Françoise Le Hingrat, Ifremer, Brest

Hydrographic Service ships have been equipped with ADCP: "Pourquoi-Pas ?" and "Beautemps-Beaupré". Collected during valorized transits or deep ocean cruises, the ADCP data are transmitted to and managed by the National Oceanographic Data Centre for France (SISMER, IFREMER) from the processing to the quality control, the archiving and the data dissemination.

Data transmission

The raw data from ATALANTE, SUROIT and THALASSA are transmitted to SISMER at the end of each cruise, whereas those from Pourquoi-Pas? and Beautemps-Beaupré are transmitted to SISMER each day in real time.

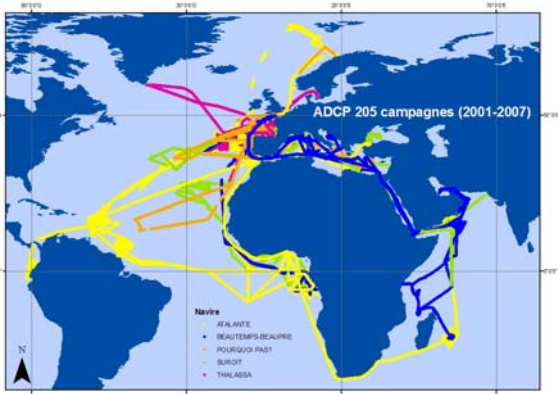


Figure 1: Data distribution

Data processing and quality checks

Once the data are received by SISMER, they are processed cruise per cruise using a software named CASCADE [1] (collection of Matlab routines), developed at IFREMER by the Laboratory of Physical Oceanography. The different steps of the data processing are:

- Reformatting of the raw binary data files into NetCDF files,
- Generation of processed files (attitude and time corrections, calculation of terrestrial coordinates, filtering, means),
- Automatic and visual quality checks of the data,
- Data presentation along a particular section,
- Error detections at the beginning of data processing or after data processing.

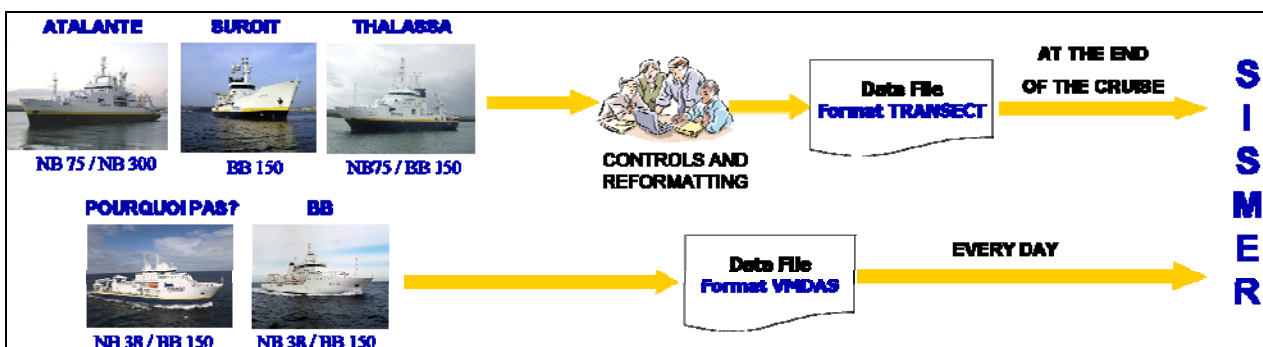
Data archiving and access

Currently, the data of about 200 cruises carried out between 2001 and 2007 are archived and are directly downloadable on the SISMER portal (under Data access http://www.ifremer.fr/sismer/index_UK.htm).

For each cruise, different files are available:

- NetCDF data files - Raw data and processed data (Date/time, Latitude, Longitude, Depth, N/S, E/W, Vertical current speed, Echo intensity).
- UNIX tar file containing figures (section map, images and vector plots of the sections).

Report which contains information about data collection, quality checks, processing procedures applied to data and problems encountered with the data.



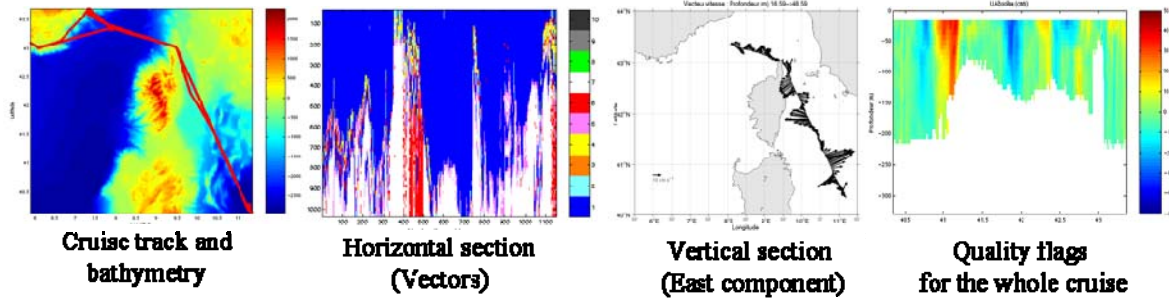


Figure 2: Examples of figures provided in the tar files

References: [1] Kermabon, C. et F. Gaillard, 2002: CASCADE, logiciel de traitement des données d'ADCP de coque. Version 3, Rapport LPO 00-03, 90 pp.

Progress in Argo Delayed Mode Quality Control

Christine Coatanoan & Virginie Thierry, Ifremer, Brest

A third DMQC workshop has been hosted in Seattle in September 2008. The driving requirement on DMQC is to ensure a high-quality product by adopting consistently-applied procedures, and ensuring timely flow of D files from all national programs to the GDACs. So, beside the core issues that remain at the heart of Argo DMQC (correction of the salinity or pressure sensor drifts for instance), additional topics were addressed:

- How to ensure that all DM operators apply DMQC procedures consistently?
- What are the known instrument errors and sensor failure modes? This knowledge is mandatory to avoid making invalid adjustments to data and to enable interaction with manufacturers to stimulate hardware and software improvements to the floats.
- The maintenance of the best possible reference datasets for evaluation of new float data.

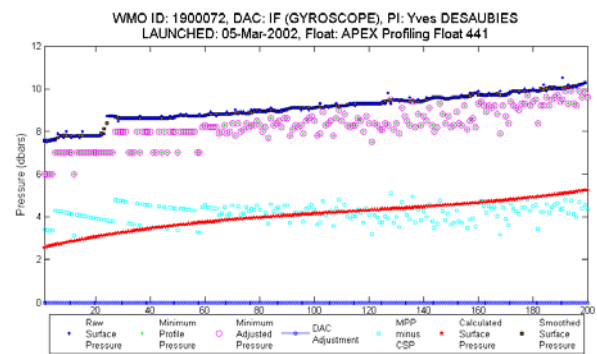
A report on this workshop is available on the Coriolis web site at: http://www.coriolis.eu.org/cdc/argo_rfc.htm.

In this report, the known instrument error and sensor failure modes are reviewed, as well as the quality control of each parameter. Some details about this quality control are provided below. Progresses on the reference databases (CTD and Argo) used for calibrating salinity data are also given in the report and detailed hereafter.

Pressure

The AST pressure working group has proposed DMQC adjustments to PRES using SURFACE_PRESSURE in APEX floats. SOLO and PROVOR floats make profile-by-profile adjustments for surface pressure measurements, by resetting the pressure offset in each profile. APEX floats do not. The problem is APF8 floats that truncate and discard negative offsets. APF-8 APEX floats with Druck sensors remain undecided. From DMQC3 and ADMT9 meetings, it has been decided that pressure will be corrected according to some criteria defined by Annie Wong and proposed to the Argo community. The steps to follow will be soon described in the

Argo quality control manual and each PI is encouraged to take care of this correction.



Example for the float 1900072 (Coriolis)

Pressure offsets in Coriolis Apex floats are investigated by Ifremer (by the Physical Oceanography Laboratory from Brest (LPO) in collaboration with Coriolis within the CREST ARGO project funded by the Brittany region) and the results are currently discussed and compared to that obtained by P. Barker from CSIRO who has been investigating pressure offsets in APEX floats from all DACs. Some information about CSIRO float diagnostics can be found at:

http://www.marine.csiro.au/~cow074/quota/argo_offsets.htm.

Salinity

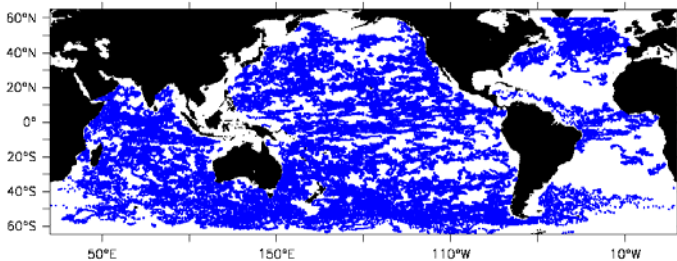
Concerning delayed-mode QC and adjustment of PSAL, efforts must be done on the conductivity sensor error termed "thermal inertia lag". Salinity reported immediately after a float has crossed a strong thermal gradient can be in error as a result of conductivity cell thermal mass. More efforts must be done to correct this kind of error for floats located in area with strong thermal gradients. A routine is already provided to correct this problem, but it has to be used with care as additional tests on the APEX ascent rate and on the PROVOR floats must be done to fully validate the proposed correction.

Temperature

No correction is at this time proposed for the temperature for which the sensor does not show known problem. Nevertheless, when PSAL drifts towards higher salinity compared with reference, the assumption of a problem with the temperature sensor can be admitted since there is no physical explanation of why conductivity cells would drift higher conductivity. If some operators find this kind of anomaly, it will be very helpful to inform the Coriolis Data Center in order to better understand and analyze the problem.

Reference database

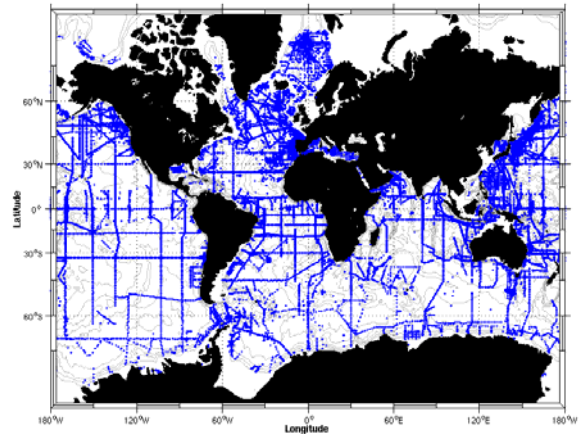
A version of CTD reference database with ITS90 unit temperature (done at Coriolis) and Argo climatology (done by John Gilson, Scripps) have been provided to DM operators. Those both databases are available on the Coriolis ftp site. A login and password are provided by asking to codac@ifremer.fr. Updates of those both databases will be done on a regular base.



Argo climatology

DMQC in regional area

Interactions with real-time QC, regional QC & the GDACs, need to be improved. To work on this way, a table showing information by regional area will be soon available on the Coriolis web site. This table will give information about area location, spatial and temporal scales, comments, link, etc.... and will be very helpful for running the OW method on floats deployed in regional areas already described in this table but also to further understand the behavior of the floats and improve the QC in real time.



CTD reference database

The 3rd Argo Science Workshop in China: the Future of Argo



The Third Argo Science Workshop (ASW-3) will be hosted by the Second Institute of Oceanography in Hangzhou, China, 25-27 March, 2009. The purpose of the meeting is to assess the general utility of the Argo array and its future direction thought the following topics:

- Heat and salt budgets on global to regional scales.
- Seasonal to inter-annual variability as seen by Argo.
- The role of Argo in constraining Ocean Data Assimilation fields.
- Estimation of circulation fields on global to regional scales.
- New technology - this might include changes to the operation abilities of a float, the addition of new sensors and other topics that might arise.

For more information:

http://www.argo.ucsd.edu/FrASW-3_abs.html



IN-SITU Delayed Mode at Coriolis Data Center: 1990-2007 Reference dataset

Cécile Pertuisot, Emilie Brion, & Christine Coatanoan, Ifremer, Brest

Since 2005, the operational analysis system set up by the Coriolis Data Center produces mainly temperature and salinity vertical profiles, but also gridded fields in near real time. This system contributed in 2007, to release a new product for operational oceanography to perform re-analysis for the global ocean over the period 2002-2006 on a delayed mode basis. One year later, these re-analysis have been enlarged to create the 1990-2007 Reference Dataset. Its main goal is to improve the database content and strengthen the quality control to fit the level required by the physical ocean re-analysis activities.

Quality Control Process

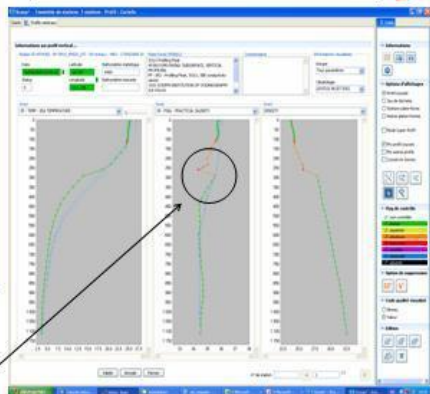
The new procedure has involved an objective analysis method (statistical tests) with a visual quality control (QC) on the suspicious profiles. The Coriolis Data Center processes temperature and salinity profiles in both real-time and delayed mode using a three-step method. It operates automatic tests, statistical tests and a visual control:

Automatic tests:

1. Platform identification
2. Impossible date test
3. Impossible location test
4. Position on land test
5. Impossible speed test
6. Global range test
7. Regional range test
8. Pressure increasing test
9. Spike test
11. Gradient Test
12. Digit rollover Test
13. Stuck value test
14. Density inversion
15. Grey list
16. Gross salinity or temperature sensor drift
17. Frozen profile
18. Deepest pressure test

Statistical tests:

- Comparison to climatology with neighbours
- Comparison to neighbourhood.



Flag manually assigned

Objective Analysis Method

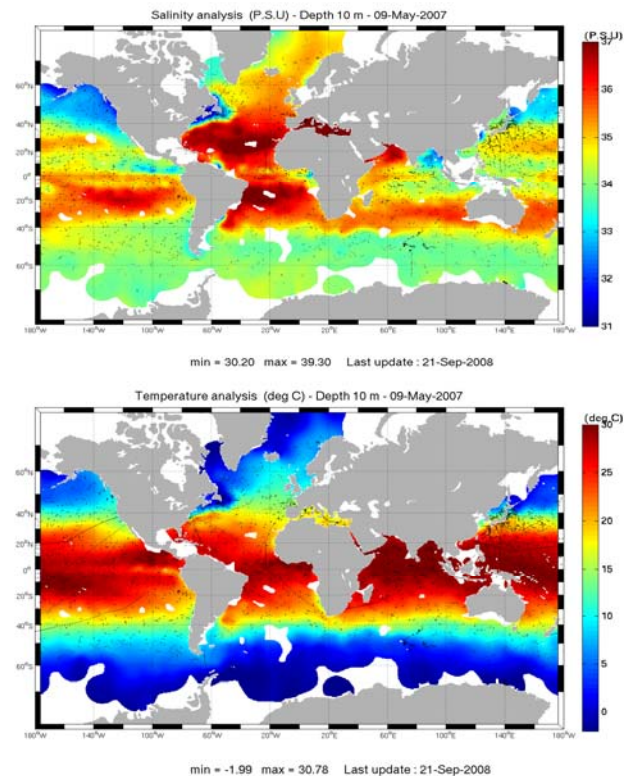
The quality control process uses two runs of objective analysis, corresponding to two different time windows, with an additional visual control in between. The first run is done on a six weeks window (t-21, t+21) to capture the most doubtful profiles and operated on a monthly basis. The doubtful profiles are afterwards visually checked by an operator to decide whether or not they are bad data or real oceanic phenomena. A quality flag is manually assigned by an operator and included in the product.

The second run is also done on a six weeks window but operated on a weekly basis for the modeling needs.

Reference Dataset 1990-2007

The reprocessing of the 1990-2007 period is a global and annual delayed analysis of the database content and an additional validation of the dataset collected in real time and delayed mode over this period. The release 2008:

- uses all type of in-situ data (ARGO profilers, XBT, CTD, Drifting Buoys, Moorings) including the updated CTD Levitus set (WOD 2005).
- provides T and S weekly gridded fields and individual profiles both on their original level and interpolated level (grid 1/2° and 59 levels).



This new 1990-2007 Reference Dataset is available on different servers using different technologies (ftp, OPeNDAP and web). For more informations, please contact our assistance at codac@ifremer.fr and check:

http://www.coriolis.eu.org/cdc/global_dataset_release_2008.htm.

Real time data are also available through our ftp, please contact also codac@ifremer.fr.

First Success of ProvBio floats

Serge Le Reste, Xavier André (1), Hervé Claustre, Fabrizio D'Ortenzio & Antoine Poteau (2)
 (1) Ifremer, Brest, France ; (2) Laboratoire d'Océanographie de Villefranche, France

The anthropogenic greenhouse effect and the associated temperature rise of the planet represent the main challenging issue for the Earth sciences of the next century. Marine ecosystems are a key component of the Earth system, as they modulate the transfer of greenhouse gases (mainly CO₂) to the ocean surface. Moreover, oceanic ecosystems mitigate the effects of anthropogenic carbon injection into the atmosphere, via the so-called "biological pump". Ocean biogeochemistry is hence confronted to a major challenge: the determination of the extent and efficiency of the climatic feedback of the carbon "biological pump" within the context of climate change.

However, the approaches currently utilized to assess ecosystem dynamics are inadequate for addressing climate change issues:

- manifestly, ocean biogeochemistry lacks observations. The number of in situ biogeochemical observations is 2-3 orders of magnitude lower than the number of observations for the physical compartment. Moreover, large areas of the ocean are practically under-sampled, as adverse environmental conditions and logistics prevent the conduction of oceanographic cruises for most of the year. Ocean color satellites have greatly improved the knowledge of biomass distribution, although they are limited 1. to the biological compartment only 2. to the surface and near surface layers.
- the temporal variability of the main processes of marine ecosystems ranges from hourly to decadal scales, showing a continuum of scales, which is extremely hard to discriminate without dedicated observations; very few oceanic regions have been sufficiently explored to allow both long-trend and high-frequency analysis, thus most of the feed-backs between processes occurring at different temporal scales are very poorly characterized.
- numerical simulations, which represent an essential tool to dissect scales and provide future scenarios, begin to produce realistic results. However, models are still far from obtaining the expected accuracy, as they are inadequately constrained by observations.

Autonomous measuring platforms represent the "deus ex machina" to unblock the impasse. They could solve all the present limitations, opening novel pathways for the exploration and comprehension of oceanic ecosystems. Physical oceanography has already cumulated huge benefits from the use of autonomous measuring platforms (i.e. Argo program). It shows the way to follow for biogeochemical ocean sciences, which should evolve towards autonomous systems in order to enhance their observation capacity.

A new type of float, the "ProvBio", has been developed jointly by Ifremer and the French company KANNAD, following the scientific directives of the Oceanographic Laboratory of Villefranche (LOV). The ProvBio design has been achieved from the Provor-CTS3 float, adding miniaturized, low power consumption, and quite neutrally buoyant optical sensors for biogeochemical measurements delivered from Satlantic and Wetlabs manufacturers. Two different models have been developed: the first, ProvBioA, is fitted with a Wetlabs transmissometer (C-Rover), a 3-wavelength Satlantic radiometer (OCR-504) and the PROVOR-CTS3 CTD sensor.

The second model, ProvBioB, comprises the same ProvBioA sensors, with, in addition, an "ECO3" Wetlabs sensor, measuring chlorophyll-a fluorescence, coloured dissolved organic matter and particle backscattering coefficients.

The ProvBioA sampling cycle is practically the same as for a classical Argo float, with the important difference that the sampling strategy can be modified in real-time (see later). The ProvBioB has an additional characteristic: the internal software allows a sampling protocol with 3 profiles per day (the surfacing times can be programmed by the user in the mission parameters, see figure 1).

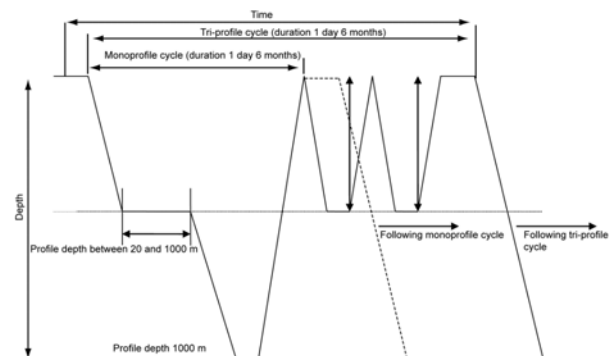


Figure 1. Diagram showing a typical ProvBioB cycle.

In the ProvBio series, the satellite communication device is based on an Iridium "two-ways" link¹, which replaces the Argos system of the Provor-CTS3, as required by the increased quantity of data to be transmitted. The Iridium "two-ways" system also allows for a real time modification of the mission parameters, by adapting, for example, the float's sampling strategy to specific events (i.e. phyto-plankton bloom, extreme wind forcing, mixed layer deepening etc). Moreover, a "mission end" command can be transmitted to the float, which gives the possibility to recover the instrument in cases of energy drops or instrument anomalies².

The housing of the optical sensors is mounted onto the main hull of the float, connected by the lower part of the housing. The optical device housing is fixed at the damping disk of the float, with 2 band clamps and contoured saddles, in order to ensure the correct alignment of the transmissometer optical path. The electrical connection with the float is assured by a cable mounted on the lower end cap (see figure 2).

A new antenna has been specifically developed for the satellite transmission system of the ProvBio series (max depth attested: 210 bar pressure).



¹ A "two ways" communication allows not only the transmission of the data from the float to land, but also the transmission of messages from land to the float.

² The "mission end" command will force the float to rejoin the surface and to transmit the position every hour.



Figure 2: The ProvBio and its deployment

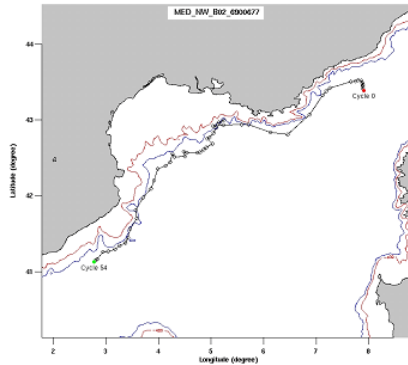


Figure 3. Geographical locations and trajectories of the of NW_B02 ProvBioB float : deployment (red dot), profiles (black dots), current position (12 December 2008, green dot). See also: www.obs-vlfr.fr/OAO.

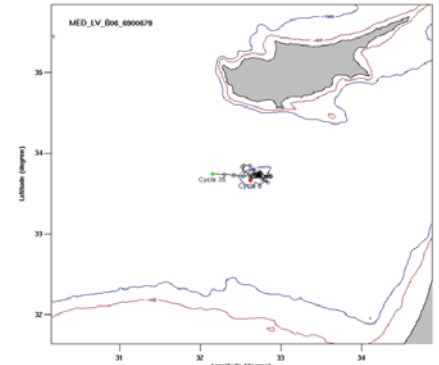


Figure 4. Geographical locations and trajectories of the LV_B06 ProvBioB float: deployment (red dot), profiles (black dots), current position (12 December 2008, green dot). See also: www.obs-vlfr.fr/OAO.

A hard coated aluminium mast maintains the antenna sufficiently distant from sea-surface (about 20 cm). The modem, from Nal research, includes a GPS receiver and an Iridium transmitter, and is located in the main hull of the float, close to the electronics pcb. The collected data are transmitted in a unique "data message" of 1960-bytes size, which comprises 14 data packets of 140 bytes each. If an error is detected, the number of packets in a message is lowered, and a new transmission is attempted. A "status message", containing technical parameters on the state of the float and of the sensors, is also separately transmitted. The transmission period at the surface doesn't exceed a few minutes, which minimizes the transmission cost and the risk of boat collisions (which depends of surface time).

A 800 cm³ foam has been fixed on the top of the float, around the hull, in order to compensate the weak negative buoyancy of the optical sensors and then to ensure a correct surfacing, which is crucial to correctly establish the satellite communication.

The optical sensors are activated 5 minutes before the start of the profiling phase (depth data are transmitted and used as "reference" values), as, to save energy, optical sensors are switched off for most of cycle period. The collected data are vertically averaged to minimize the transmission cost, although the efficiency of the Iridium system allows a rather metric resolution (about 2 meters). This is also done for CTD derived parameters. If the "three-profile" option is selected, all the data from the 3 profiles are transmitted at the end of the third profile. The assessment of ProvBioB lifetime is of about 200 "one-profile" cycles and of about 100 "three-profile" cycles³¹.

At present, 4 ProvBioA and 8 ProvBioB have been manufactured and 2 other similar floats, named ProvCarbon (with transmittance and oxygen sensors) are also being produced. Concerning the ProvBioB, all 8 floats have been delivered to the LOV for science operations. They have been successfully deployed and all are presently operational: 2 in the North Atlantic (from June 2008), 2 in the North Pacific near Hawaii (from august 2008), 2 in the South Pacific (from December 2008) and 2 in two ecological contrasting regions of the Mediterranean Sea.

³¹ With the following assumptions: 1000 meter profiling depth, 52 CTD samples and 150 optical samples (e.g. 1 point every 2 m between 300m depth and surface).

The first Mediterranean float (NW_B02) was initially deployed the 1st May 2008, in the Ligurian Sea, close to the French long term in situ optical mooring BOUSSOLE (P.I. D. Antoine, approximately 8°E, 43.5°N, see figure 3). The float was programmed with a cycle frequency of 1 day. After 15 days, the cycling frequency was changed to 5 days, and it was kept constant until now.

The second float (LW_B06) was deployed in the Levantine Basin (approximately 32.5°E, 33.7°N, see figure 4), during the French cruise "BOUM" (P.I. Thierry Moutin). The LV_B06 float was programmed similarly to the NW_B02: after an initial phase at 1 day cycling frequency (from 27/06/08 to 30/06/08), the float strategy was modified to perform 5-day cycling.

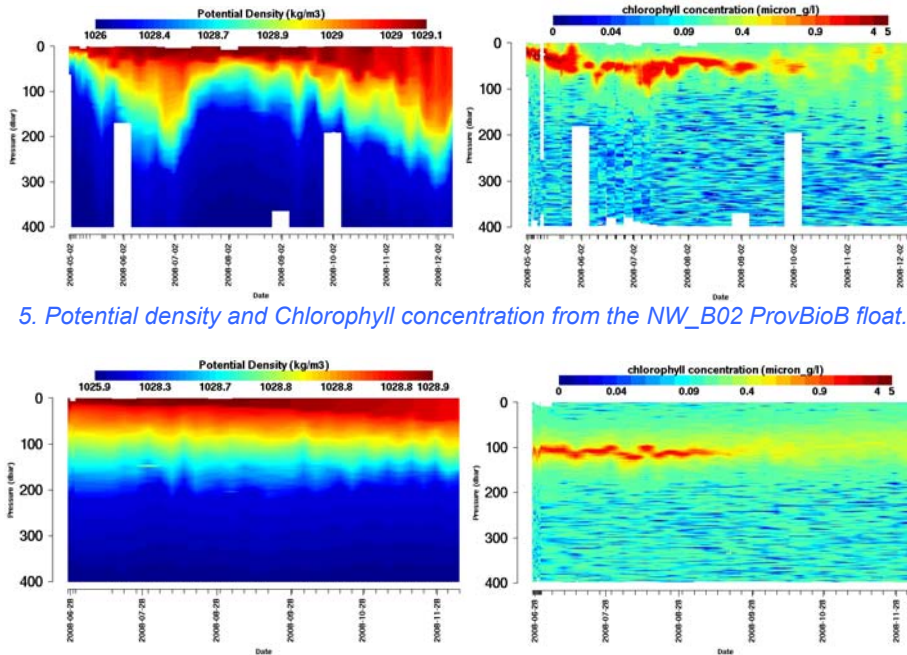
Figure 5 shows the temporal evolution of the potential density and of the chlorophyll concentration fields obtained from the NW_B02 ProvBioB float. The summer stratification of the water column affected the vertical distribution of the chlorophyll concentration, which was then characterized by a Deep Chlorophyll Maximum (DCM) at about 50-70 meters depth. The beginning of the fall in September, with the associated atmospheric cooling and the more intense wind mixing, induced a progressive deepening of the mixed layer depth, with a consequent de-stratification of the water column. As winter advanced, the DCM was progressively destroyed, and the chlorophyll concentration was redistributed uniformly in the mixed layer by the intense mixing.

Dynamical conditions of the LW_06 float are relevantly different (see figure 6). The float, as initially expected, remained trapped in the cyclonic structure related to the Eratosthenes seamount, and it profiled the same area for most of the summer and fall. The summer stratification was more important than in the Western Mediterranean basin, and, although winter conditions were observed, the mixed layer depth was never greater than 50 meters. Consequently, a DCM was permanently observed at about 100 meters depth, although the characteristics of the vertical profiles of the chlorophyll concentration varied between summer and winter. The absolute values of chlorophyll-a concentrations, ways observed in the DCM, tended to decrease with time, ranging from 1-2 mg/m³ in the summer to 0.5-0.7 mg/m³ in the fall.

The two Mediterranean ProvBioB's are still operational (December 2008), and their evolution can be followed in real-time on the LOV web site (www.obs-vlfr.fr/OAO), as

transmitted data are processed and plotted on the web site with a temporal delay of less than an hour. A Group Mission Mercator Coriolis project (PABIM, P.I. Fabrizio D'Ortenzio) is presently dedicated to the definition of an automatic quality control processing for the ProvBio observations, which will be in the future integrated in the Coriolis data system. Technical monitoring of the floats indicates that the energy level is still high, therefore a complete annual cycle of measurements remains possible.

In conclusion, the firsts two Mediterranean ProvBioB have produced, in less than a year, an invaluable data set on physical-biological interaction in two contrasting ecological regions of the basin. Considering the quality of the data, the cost/benefits ratio for this first ProvBio experiment is extremely favourable.



5. Potential density and Chlorophyll concentration from the NW_B02 ProvBioB float.

Figure 6. Potential density and Chlorophyll concentration from the LV_B06 ProvBioB float

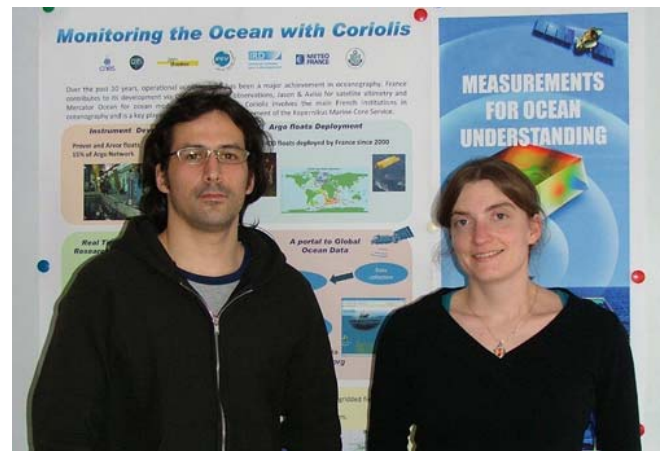
A scientific team for the Coriolis Project

C. de Boyer Montégut¹ & C. Cabanes²

¹ Laboratory of Oceanography from Space (LOS), Ifremer, Brest - ² CNRS, DT INSU, Ifremer, Brest

As operational oceanography grew up at the end of the 90's, the need for a strong support concerning its observational part became more important. The Coriolis project was launched in order to contribute to the ocean in situ measurements part of the French operational system. The success of Coriolis in developing continuous, automatic, and permanent observation networks and providing high quality observation data for forecast models, especially for Mercator, has been demonstrated since then.

The ocean model needs the highest quality data possible as the constraints of those data in the assimilation system can be quite influential for the final results. The data may especially take the model away from a realistic state by introducing artefacts like, for example, drift or biases in a temperature or salinity profile. Direct use of in-situ observation data for research purposes also requires some preliminary advanced qualification tests. Some recent examples of the problems encountered in in-situ data accuracy are the cold bias of a group of SOLO Argo floats in the Atlantic (Willis et al., 2007), or the deep warm bias of XBT



Clément de Boyer Montégut & Cécile Cabanes

measurements (e.g., Wijffels et al., 2008). Those problems could be evidenced while trying to evaluate oceanic temperature climatic trends. An efficient way to know about

data potential problems is to treat and analyze those observations for scientific purpose. Coriolis project also aims at growing towards an international level (Euro-Argo and MyOcean). In those perspectives, a new step has been done by creating a scientific team in the frame of the Coriolis project. This team represents the scientific component of the project whose two others are data measurements and acquisition, and data management in Coriolis data centre at Ifremer, in Brest. While external scientists will continue to be there to assist, give advice and help for this project (Gilles Reverdin, Cnrs; Yves Gourriou, Ird), an Ifremer researcher (Clément de Boyer) and a Cnrs research engineer (Cécile Cabanes) have been hired since end of 2008. Two postdocs (Claire Gourcuff and Karina Von Schukman) and a PhD student (Mathieu Hamon) also arrived to participate to Coriolis research activities.

The main goal of this group, as stated in the 2009-2012 convention signed by the seven funding agencies (ifremer, cnrs, cnes, ird, ipev, meteo-france, shom) is to process, analyse and enhance the value of the data managed by Coriolis data centre and more generally to be the scientific support of the project. Three main lines will be followed in the work of Coriolis scientific team:

- advice and strategy : An important task of this part will be the support to Coriolis data centre through the development of new methods improving data quality and their transfer to the centre (work in collaboration with Loïc Petit de la Villéon, Christine Coatanéoan and Thierry Carval from Coriolis data centre). Other tasks will be to drive internships and scientific external contracts, give advices for research axis (especially in the frame of Coriolis-Mercator Mission Group), and follow and guide the float improvements and their deployment strategy.
- validation and qualification: work on new methods to improve data quality and make the associated documentation, in order to make it operational by the data centre.
- valorisation of the data through analyses and generation of new products aimed to help solving research issues : An example of this work is the careful estimation of new atlases (sst, sss, mixed layer depth, heat content...) and climatic indices (niño3.4 index, Indian ocean dipole index...) from in-situ observations. Analyses of the data will also be conducted in order to answer scientific questions like for example quantifying and understanding the amplitude of long term temperature change in the oceans. The data and products established here will be made available to the research community through internet (see end of the text for web address).

For its activities, the Coriolis scientific team may rely on collaborations with researchers from other laboratories in France, Europe and abroad. The team should also get feedbacks about the data from a user group in order to be reactive on potential problems of the data and eventually enhance their quality.

A plan of activities for the coming year has been done and we can give here the main points of it. We present first some activities concerning the validation and qualification of the data. An additional consistency test has just been transferred to the data centre and will help to detect outliers presenting large discrepancies with a reference climatology or comparing group of floats with each other. A task will be

dedicated to help in the processing of delayed mode Argo data, by giving some advices and assistance on how to treat some floats without PIs or whose PIs cannot take care of. Later this year the issue of correction of surface pressure drift on Apex will be addressed. An important task is to validate the new COriolis Re-Analysis (CORA) product designed for global ocean circulation reanalysis and research purposes. It is an extract of all available in-situ data at Coriolis data center at a certain date, that Coriolis team (data center and scientific team) qualifies as well as possible in order to make it ready to use by the forecasting centers or research teams such as the GLORYS project for example. One important point to tackle is the correction of XBT data drop rate errors that introduces some warm bias at depth. Some work has already been done in the frame of Mathieu Hamon PhD and the corrections should be done by May or June of this year. Other works that will be conducted concern the operational validation of thermosalinograph data from research vessels which will be processed according to the TSG quality control procedures currently done by the IRD.

Concerning the valorisation and analyses of data, some projects are also planned or already in course. An atlas of Barrier Layer Permeability will be made available with an associated paper (Mignot et al., 2009). A work is currently done to evaluate as precisely as possible the Argo displacement velocity at depth and make an atlas of it, available for end of March or April (collaboration with Michel Ollitrault, LPO, Ifremer). Some collaboration is also active in the frame of Mercator-Coriolis Group Mission projects like PABIM (Fabrizio d'Ortenzio, LOV, Cnrs), or PROSAT (Louis Prieur, LOV, Cnrs). Those projects goals are respectively to estimate biogeochemistry activity from Argo floats (and for example understand the links between biogeochemistry and ocean physical parameters like mixed layer depth), and try to estimate the mixed layer depth from both in-situ and satellite data. Another example of scientific project that started recently is the colocalisation of Argo data with tropical cyclones in order to describe and understand the influence of the ocean in the ocean-atmosphere coupling processes at play in those important climatic phenomena (collaboration with Matthieu Lengaigne, LOCEAN, Ird).

The data and products aimed for research and developed in Coriolis scientific team in collaboration with the data centre will be made available shortly on the web (CORA, atlases, climatic indices...). A link to those pages will be given soon on Coriolis website <http://www.coriolis.eu.org/>.

References :

- Mignot, J., C. de Boyer Montégut, and M. Tomczak, 2009: On the permeability of Barrier Layers, to be submitted to Ocean Science.
- Wijffels, S.E., J. Willis, C.M. Domingues, P. Barker, N.J. White, A. Gronell, K. Ridgway, and J.A. Church, 2008: Changing Expendable Bathythermograph Fall Rates and Their Impact on Estimates of Thermocline Sea Level Rise. *J. Climate*, 21, 5657–5672.
- Willis, J. K., J. M. Lyman, G. C. Johnson, and J. Gilson (2007), Correction to "Recent cooling of the upper ocean", *Geophys. Res. Lett.*, 34, L16601, doi: 10.1029/2007GL030323.

SSS-fronts properties deduced from TSG data in the North Atlantic Subpolar Gyre

Agnès Desprès and Gilles Reverdin, LOCEAN, Paris

The western part of the North Atlantic subpolar gyre is the site of intense air-sea interaction resulting in episodic deep convection in certain areas of the Labrador Sea, but also sometimes in the Irminger Sea (Pickart et al., 2003). In this region, surface water of different origins (subtropical, subpolar or from the Arctic) is brought by an intense cyclonic circulation and its eddies, and is transformed into deeper water either near the convection sites or by entrainment of dense overflows over sills separating it from the Nordic Seas. The large-scale circulation is expected in some instances to separate the different water masses that will form fronts near particularly intense currents. It is also expected that in the presence of large scale gradient of surface properties (in this instance, usually cooler and fresher towards the west), an eddying ocean will be associated with numerous fronts resulting from the variability and the confluence patterns (Klein et al., 1998).

We are seeking to identify these fronts, their distribution and properties in surface data. Furthermore these fronts can modulate the air-sea interactions due to atmospheric response to mesoscale surface temperature variability, and therefore the mixed layer properties and water mass characteristics on those scales. For this investigation, we mostly relied on a set of more than 10 years of ship-of-opportunity thermo-salinograph (TSG) data, as well as on the mapped currents produced by AVISO from altimetric satellite sea level data and a climatology of the surface currents (Rio and Hernandez, 2004). The TSG data were collected on two lines, one between Denmark and west Greenland with the Nuka Arctica since 1997 (NA, green on Fig. 1), and one between Iceland and Newfoundland with different vessels since 1994 (SK, red on Fig. 1). These two lines provide in all seasons a good coverage of the eastern Irminger Sea, albeit, only since 2003 in winter for NA.

Because of various difficulties on the data, in particular during poor weather, a strong screening of the data had to be applied and only data reduced by a 20 km running mean filter can be homogeneously derived throughout the time series. These data are decimated every 10 km. Fronts are then identified on the data based on a salinity gradient criteria (see Desprès and Reverdin, 2008, for details). This roughly corresponds to fronts across which the gradient smoothed over 50 km exceeds by a factor 3 an average basin scale gradient. We chose this criterium to favor fronts with scales that can also be identified in the mapped currents from altimetry, and that might not result from very local precipitation or remaining data errors. In practice the gradients are often concentrated over a smaller spatial scale. Once identified in salinity, the corresponding salinity, temperature and density gradients, as well as width are estimated. An example is provided on Fig. 2. On this plot, positive fronts will correspond to a salinity increase towards the east (same sign as the large scale SSS gradient), and the distance is referred to the section crossing of the top of the

Reykjanes Ridge (RR). We identify a negative front in the west with no associated T signal, and three other fronts also identified in S. The first two of those correspond to an eddy structure and the second and third ones have no density contrast, whereas the first one has a density contrast dominated by temperature.

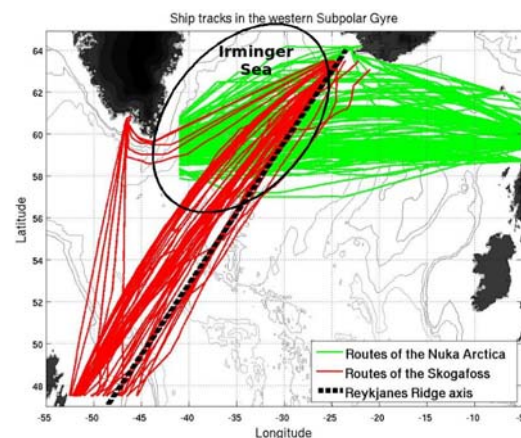


Figure 1: Nuka Arctica (green) and Skogafoss/Godafoss/Selfoss (red) tracks in the Subpolar Gyre from 1994 to 2007.

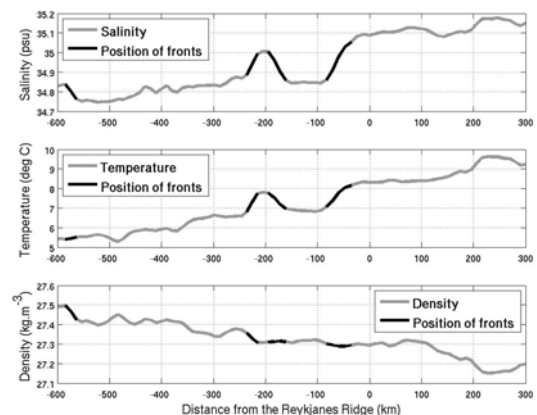


Figure 2: Hydrographic profiles on a Nuka Arctica section in November 2000 : SSS (top panel), SST (middle panel), and density (bottom panel). SSS fronts are marked in black.

Indeed, over the whole data set, most of the salinity fronts have also a temperature signature, with a minimum of associated T signatures in summer. We also tried to identify fronts from a temperature criterium, and found that except in summer, a majority of the fronts also have a salinity signature. Most of the fronts we identify in the NA data set and away from shelf-break currents or the East Greenland Current are located in the Irminger Basin, and we will concentrate on those in the following. We find more of these fronts in summer and autumn than in other seasons. We also find that the salinity, temperature and density contrasts

across the fronts present a strong seasonal cycle, and that they are closely related to the large scale S, T and density gradients across the Irminger Sea (Fig. 3). These are such that salinity gradients tend to be reinforced in summer and autumn whereas temperature gradients are larger in winter. The larger winter temperature gradients originate from the western increase in autumn/winter heat loss and associated convection linking the surface waters with the cool intermediate waters of the subpolar gyre. The increase in salinity gradients in summer and autumn might be related to the eastward transport in summer of the fresh Arctic waters originating from the shelves or the western Labrador Sea through large scale circulation and Ekman transports (Holliday, 2007). Because of these two opposite cycles, density contrast across fronts is such as to present a larger salinity contribution in summer and of temperature contribution in winter.

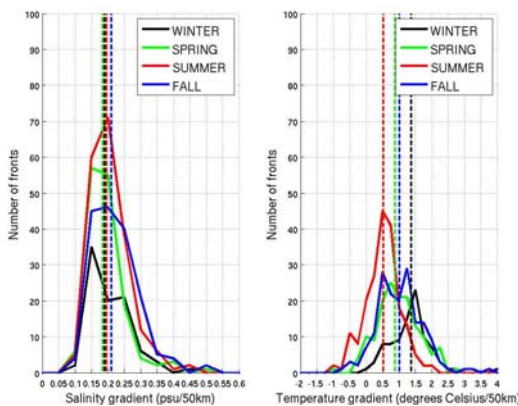


Figure 3: Seasonal statistics on positive fronts identified along the route of both ships : SSS gradient over 50 km (left panel), SST gradient over 50 km (right panel). Vertical dotted lines are medians.

This suggests that whatever the formation mechanism of the fronts, their properties basically originate from the large scale property gradients. We can also expect an air-sea modulation of properties across fronts, such as the cool side of the front be associated to a positive anomaly of air to sea heat and fresh water (less evaporation) fluxes. This would reinforce the salinity contrast across the fronts and diminish the temperature signal. This would also result in deeper mixed layers on the warm side of the fronts. Such properties are found across fronts identified in the same area and with rather similar properties across them in ORCA025 simulation G70 (Molines et al., 2006). Whether such mechanisms also take place in the real ocean will need to be further investigated with in situ data, at least for the mixed layer depths from XBT profiles also collected from those vessels.

When considering the spatial distribution of fronts (Fig. 4), we find that it is rather inhomogeneous with two peaks near 0-50 km (EIC) and 100-150 km (WIC) west of the Reykjanes Ridge, and a third maximum near 460 km in the central Irminger Basin (CIB). This distribution is also present to some extent in the ORCA025-G70 simulation. The maximum closest to the Reykjanes Ridge corresponds to an area of weak EKE in the AVISO currents, on the east side of the northeastward Irminger Current. Because there is such low EKE, this might be a region of permanent fronts separating water masses of different origins, as is also suggested in this region by the Ovide sections. The two other fronts correspond to areas of large eddy activity. WIC is located on the west

flank of the average Irminger Current, where individual current maps show the intermittent presence of the Irminger Current. CIB is in an area of weak northward circulation. Both this northward flow and EKE have increased throughout the altimetric mapped period (see Volkov, 2005).

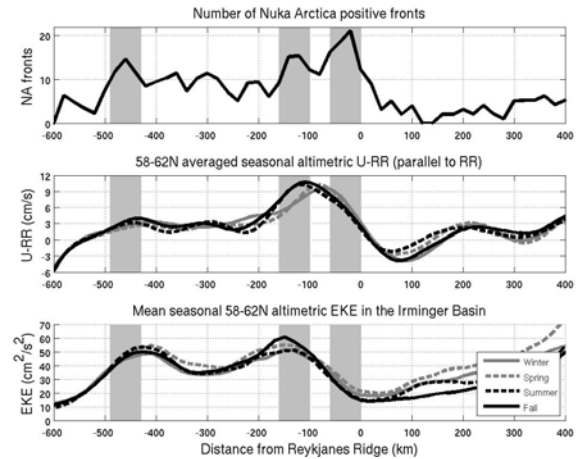


Figure 4: Number of positive SSS fronts along the Nuka Arctica track, as a function of distance from the top of the Reykjanes Ridge (top panel). Mean seasonal U-RR current (parallel to RR) computed from altimetry between 58° and 62°N (middle panel). Mean seasonal Eddy Kinetic Energy (EKE) computed from altimetry between 58° and 62°N (bottom panel). Shaded areas are locations of the three peaks of high occurrence of fronts.

To further investigate the dynamical origins of the fronts, we co-locate the fronts with the mapped AVISO currents (computing, for each front, the anomaly of the current field by removing the interannual average from the instantaneous currents, in a referential centered on the front position). We then compose those 2-D maps over all positive fronts (positive SSS gradient towards the east or north-east). This exercise done separately for the SK and NA data sets (which cross differently the currents and regions of large EKE) produce similar results that can be summarized with the NA fronts (Fig. 5). We find a difference in the circulation anomalies between the EIC and the other fronts. The EIC is associated with a northward current anomaly near or east of the front and a negative anomaly further west, suggesting that those fronts tend to be located near the core of the Irminger Current, which maximum is found further west at other times. The other fronts are associated with a dipole eddy anomaly structure, a maximum positive anomaly (and northward current) centered on the front, and anticyclonic/cyclonic eddies to its east/west (warm-salty/cold-fresh side). The only difference with SK is that identified anomalies are shifted in the direction perpendicular to the ship's route (NE-SW). Those characteristics suggest that the origin of these fronts could be in local confluence patterns and variability associated with meso-scale eddies. This would need to be further investigated with more sophisticated dynamical tools as the Finite Size Lyapunov Exponents of d'Ovidio et al., (FSLEs, 2004).

The other fronts are associated with a dipole eddy anomaly structure, a maximum positive anomaly (and northward current) centered on the front, and anticyclonic/cyclonic eddies to its east/west (warm-salty/cold-fresh side). The only difference with SK is that identified anomalies are shifted in the direction perpendicular to the ship's route (NE-SW).

Those characteristics suggest that the origin of these fronts could be in local confluence patterns and variability associated with meso-scale eddies. This would need to be further investigated with more sophisticated dynamical tools as the Finite Size Lyapunov Exponents of d'Ovidio et al., (FSLEs, 2004).

Conclusions

The TSG data we used have been very valuable to identify surface fronts across a large part of the North Atlantic subpolar gyre. Key to it has been a large number of sections through all the seasons and a thorough screening of the data, in particular in salinity. The data, with the addition of a few additional data, in particular from profiling floats are nearly sufficient to track the inter-seasonal variability in large scale salinity and temperature (although temperature anomalies are associated with remaining biases when there was no intake sensor and for periods with weak flow through the TSG). However, the data are not sufficient to track the variability in front positions, because a significant part of the fronts seem to be associated to transient features associated with eddies and which are therefore not very well sampled with the sporadic crossing of the vessels equipped with TSGs. The support of realistic model simulations or ocean reanalysis products resolving the meso-scales will be necessary to investigate this further.

We have not addressed the vertical scales of the fronts, and how the surface fronts might deviate from or be aligned with subsurface fronts. Well-sampled repeated hydrographic sections as the Ovide sections (Lherminier et al., 2007) will be required to investigate this further. XBT profiles collected along the NA and SK lines (WOCE lines AX01 and AX02) might also contribute to clarify this issue. The Nuka Arctica also carries a VM-ADCP profiler (Knutsen et al., 2005), as well as a pCO₂ sampler. Jointly analyzing these data might provide further information on the fronts and in particular the air-sea interactions taking place in their vicinity.

References:

- Desprès, A., and G. Reverdin, 2008: Surface fronts in the North Atlantic Subpolar Gyre. Submitted to J. Phys. Oceanogr.
- Holliday, N.P., A. Meyer, S. Bacon, S.G. Alderson, and B. de Cuevas, 2007: Retroflexion of part of the east Greenland current at Cape Farewell. *Geophys. Res. Lett.*, 34, L07609, doi:10.1029/2006GL029085.
- Klein, P., A.M. Tréguier, and B.L. Hua, 1998: Three-dimensional stirring of thermohaline fronts. *J. Mar. Res.*, 56, 589-612.
- Knutsen, O., H. Svendsen, S. Osterhus, 2005: Direct measurements of the mean flow and eddy kinetic energy structure of the upper ocean circulation in the NE Atlantic. *Geophys. Res. Lett.*, 32, L14604, doi:10.1029/2005GL023615.
- Lherminier, P., H. Mercier, C. Gourcuff, M. Alvarez, S. Bacon and C. Kermabon, 2007: Transports across the 2002 Greenland-Portugal Ovide section and comparison with 1997. *J. Geophys. Res.*, 112, C07003, doi: 10.1029/2006JC003716.
- Molines, J.M, B. Barnier, T. Penduff, L. Brodeau, A.M. Tréguier, S. Theetten, and G. Madec, 2006: Definition of the interannual experiment ORCA025-G70, 1958-2004. LEGI report, LEGI-DRA-2-11-2006, available at <http://www.ifremer.fr/lpo/drakkar>.
- Pickart, R.S., F. Straneo, G.W.K. Moore, 2003: Is Labrador Sea Water formed in the Irminger Basin? *Deep-Sea Res.*, Part I, 50, 23-52.
- Rio, M.H., and F. Hernandez, 2004: A mean dynamic topography computed over the world ocean from altimetry, in situ measurements, and a geoid model. *J. Geophys. Res.*, 109, C12032, doi:10.1029/2003JC002226.
- Volkov, D.L., 2005: Interannual Variability of the Altimetry-Derived Eddy Field and Surface Circulation in the Extratropical North Atlantic Ocean in 1993-2001. *J. Phys. Oceanogr.* 35, 405-426

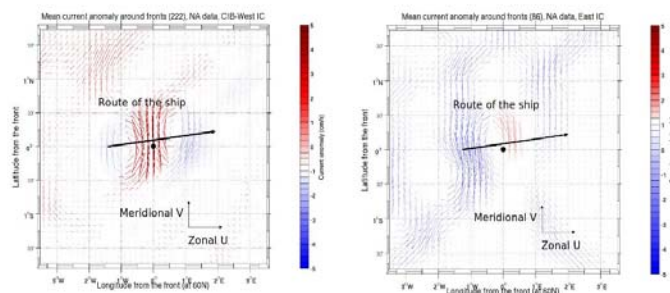


Figure 5: Mean 2D-current anomalies around NA positive fronts: in the center of the Irminger Basin and western part of the Irminger Current (left panel), on the eastern flank of the Irminger Current (right panel). Pictures are centred at the front, which is marked by a black dot. The route of the ship is drawn as a black arrow, and the coordinate system is also shown (red colour for currents with a northward meridional component, blue colour for currents with a southward meridional component).

Acknowledgments

The TSG installation and sampling programs are supported in France by INSU (SO SSS) with technical support of IRD US IMAGO (D. Diverrès) and by NOAA. The analysis of the data is supported by the Ovide LEFE project, and the collection of validation data by numerous observers and crews of the vessels, as well as with the support of the Marine Institute in Reykjavik (HAFRO) & the Greenland Department of Environment. We are very grateful to the shipping companies EIMSKIP and Royal Arctic Lines for their unconditional support over the years. ORCA025 simulations were provided by the DRAKKAR research group. The altimeter products were produced by Ssalto/Duacs and distributed by AVISO, with support from CNES.

When satellite altimetry is called for to help on Argo quality control issues

Stéphaine Guinehut, CLS Space Oceanography Division, Toulouse, France

A new method has been developed to check the quality of each Argo profiling floats time series. It compares collocated Sea Level Anomalies (SLA) from altimeter measurements and Dynamic Height Anomalies (DHA) calculated from the Argo temperature (T) and salinity (S) profiles. By exploiting the correlation that exists between the two data sets (Guinehut et al., 2006) along with mean representative statistical differences between the two, the altimeter measurements are used to extract random or systematic errors in the Argo float time series. Different kinds of anomalies (sensor drift, bias, spikes, etc) have been identified on some real-time but also delayed-mode Argo floats. About

4% of the floats should probably not be used until they are carefully checked and reprocessed by the PIs.

Altimeter measurements are from the AVISO combined maps (<http://www.aviso.oceanobs.com>). Argo T/S profiles are from the Coriolis-GDAC data base uploaded as of Feb. 2008 (<http://www.coriolis.eu.org>). Dynamic height anomalies are calculating using a reference level at 900-m depth and a dedicated Argo mean dynamic height. When available, delayed-mode fields are preferred to real-time ones and only measurements with flag at '1' are used. Data and method are fully described in Guinehut et al., 2008.

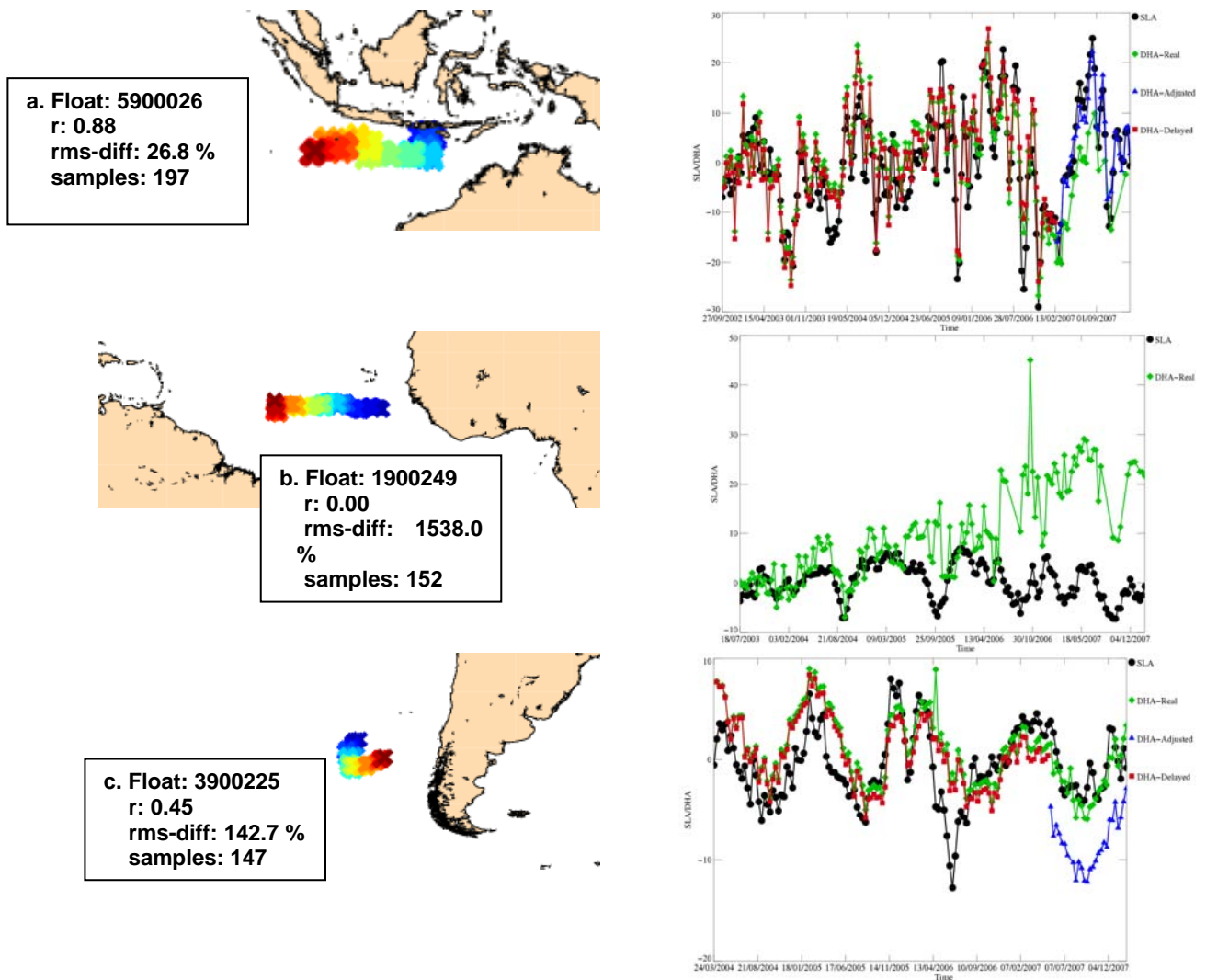


Figure 1: SLA and DHA time series for three floats (in cm). The positions of each float are also indicated, the blue cross corresponding to the deployment position and the red cross to its last reported position. The statistics correspond to r: the correlation coefficient between the two times series and rms-diff: the rms of the differences between the two times series expressed as percentage of the variance of the altimeter signal.

Some examples of SLA/DHA time series are given on Figure 1 together with the float position and its mean statistics. The WMO 5900026 float travelling from September 2002 up to the present from East to West South of the Java Island in the Indian Ocean show very good consistencies between the two time series with a correlation of 0.88. Mesoscale structures up to 25 cm are well represented in both time series and the impacts of the delayed-mode and real-time adjustments are clearly visible. The second example (WMO 1900249 float, Figure 1-b) shows clearly a progressive drift of the DHA time series regarding the SLA time series as the float is travelling from East to West in the Tropical Atlantic Ocean. Additionally, the correlation between the two time series is null, while it is expected to be greater than 0.5 (Guinehut et al., 2006, 2008) showing a clear malfunction of one of the sensor. The last example, for the WMO 3900225 float in the South Pacific Ocean (Figure 1-c) shows that part of the data have been delayed-mode control and then, the SLA and DHA time series match each other very well. At the end of the time series, when values adjusted in real time are available, they show a constant offset of about 10 cm with the altimeter data. This offset seems to be due to the salinity offset value of 0.092 applied in real-time which is with any doubt over estimated and wrong compared to the 0.015 value applied for the delayed-mode.

Results obtained for each Argo float time series are summarized on Figure 2; one point represents the value for one time series at its mean position. For most of the floats (more than 3900), rms of the differences between SLA and DHA are of the order of the referenced numbers (not shown).

160 anomalous floats with much higher values (some of the red dots on Figure 2) can be detected all over the different oceans. As illustrated by the two examples on Figure 1-b,c, these higher values are mainly the results of errors on the float time series due to a systematic offset, a spike or the drift of a sensor (salinity or pressure). More investigations on these particular floats are thus needed.

This study has demonstrated that SLA/DHA comparisons are very efficient in detecting spikes, systematic offset or drift in some Argo float time series. The comparisons also give a very quick idea of the behaviour of the time series of the float. The main advantage of this method is the use of independent and contemporaneous altimeter measurements. It appears to be very complementary to the real-time and delayed-mode Argo quality controls (Wong et al., 2008) or the use of more classical methods based on historical data sets or climatological fields. Additionally, the comparisons can be activated in near real-time in order to detect problem before the full delayed-mode quality controls but also as a verification tool after the delayed-mode control to validate it and to quantify its impact.

Finally, as part of these results has been already provided to some PIs, some floats time series might have already been corrected or separated on the GDAC data base. Also, as an on-going collaborative effort, the list of the anomalous floats and the figures of the collocated SLA/DHA time series have been published on the Coriolis GDAC web site:

<ftp://ftp.ifremer.fr/ifremer/argo/etc/argo-ast9-item13-AltimeterComparison/>.

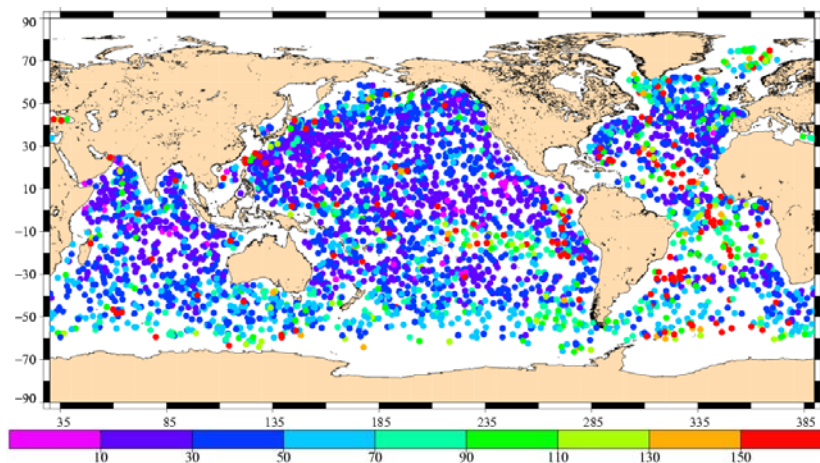


Figure 2: Rms of the differences between SLA and DHA as a percentage of the SLA variance (in %) – one point represents the value for one float time series at its mean position.

References

- Guinehut, S. P.-Y. Le Traon, and G. Larnicol, 2006: What can we learn from global altimetry/hydrography comparisons?, *Geophys. Res. Lett.*, 33, L10604, doi:10.1029/2005GL025551.
- Guinehut, S. C. Coatanoan, A.-L. Dhomps, P.-Y. Le Traon and G. Larnicol, 2008 : On the use of satellite altimeter data in Argo quality control, *J. Atmos. Oceanic Technol.*, in press.
- Wong, A. P. S., R. Keeley, T. Carval, and the Argo Data Management Team, 2008: Argo quality control manual, Version 2.31, ar-um-04-01.

Vertical variability of Near-Surface Salinity in the Tropics: Consequences for SMOS Calibration and Validation

Claire Henocq (1)(2), Jacqueline Boutin (1), Gilles Reverdin (1), Sabine Arnault (1), Philippe Lattes (1)
(1) LOCEAN/IPSL, Paris, France - (2) ACRI-St, Sophia-Antipolis, France

Introduction

Monitoring the Sea Surface Salinity (SSS) at global scale is a major challenge for the scientific community. Deployment of Argo floats, beginning in the year 2000, was a big step in improving the sampling of salinity measurements. However, although the number of active floats increases from year to year, the surface ocean coverage remains uneven and measurements are mostly deeper than 5 m depth. Synoptic and quasi-permanent surface ocean coverage is a strong argument in favour of satellite measurements. Recent technological developments concerning using L-band (1.4 GHz) radiometry will lead to the launching of the European Space Agency/ Soil Moisture and Ocean Salinity (ESA/SMOS) satellite mission in summer 2009. Its goal is to derive SSS with an accuracy of 0.2 practical salinity scale (pss) on averages over 10 days and 200 x 200 km². Given the exploratory nature of the mission and the weak sensitivity of L-band radiometric measurements to SSS, the comparisons between in situ and SMOS retrieved SSS will be a critical step to improve the calibration of the instruments and of the retrieval algorithms and to validate the retrieved SSS. However, SSS retrieved from L-band radiometry will be representative of the top first centimeter of the ocean surface, whereas in situ measurements are made at several meters depths. This paper focuses on the vertical salinity structure in the top 10 m of the ocean.

Data and Methods

The vertical salinity stratification is studied at two scales. On the local scale, thanks to TAO moorings (McPhaden, 1995), temporal evolution of salinity at 1, 5 and 10 m depth is studied in relation with rainfall events. We use hourly mean of salinity and rain rates measured every 10 minutes. At regional scale, throughout the tropical band, between 30°S and 30°N, vertical salinity differences in the first 11 m below the sea surface are studied using three kinds of in situ measurements:

TSG measurements on moored platforms at 1, 5 and 10 m (hourly mean from 13 TAO/TRITON and PIRATA moorings) and on board the R/V Polarstern at 5 m and 11 m below the surface (measured every 15 minutes). This ship crosses the Atlantic Ocean twice a year.

Argo measurements, taken from the Coriolis database. In order to avoid depth averaged salinity, only APEX measurements, are considered.

CTD and XCTD salinity measurements taken from the World Ocean Database 2005 (WOD05, Boyer et al., 2006), from SISMER database (mainly conducted in the Gulf of Guinea and to the east of Indonesia) and from the ARAMIS project (Arnault et al., 2004). For CTD and XCTD measurements, only data below 4 m are retained.

The temporal distribution extends from January 2000 to December 2006, with one exception for measurements made on the R/V Polarstern (between 1993 and 2005). To discard biased and wrong data, validation flags provided with measurements are taken into account (e.g., for Argo measurements, only data with a validation flag equals to 1 or 2 are retained) and extra verifications and corrections are made.

For each vertical profile, vertical salinity differences are ranked in three groups (in the following they are referred as vertical levels): $\Delta S_{10-5} = S[8; 11] \text{ m} - S[4; 6] \text{ m}$, $\Delta S_{5-1} = S[4; 6] \text{ m} - S[0; 2] \text{ m}$ and $\Delta S_{10-1} = S[8; 11] \text{ m} - S[0; 2] \text{ m}$, where $S[X_{\min}; X_{\max}] \text{ m}$ stand for salinity measured between X_{\min} and X_{\max} meters depth. ΔS_{5-1} and ΔS_{10-1} groups are based only on TAO/PIRATA measurements.

The influence of rainfall on vertical salinity differences is analyzed using rain rates derived from SSM/I, TMI and AMSR-E satellites. Satellite instruments provide two instantaneous "snapshots" each day but no indication on the start time of the rain event, its duration, and its overall intensity. As we expect that the rain history will influence the sea surface freshening, a rain parameter called the "3-day maximum accumulation rain rate" (3d max rain rate) is created. It is derived as the sum over three days of the maximum rain rate measured each day by the different satellites. Salinity vertical differences are collocated with the 3d max rain rate computed over the previous 72 hours in 25 km radii.

Vertical salinity differences

On the local scale, measurements on TAO moorings highlight a strong impact of rain on the salinity vertical stratification with a surface freshening of several tenths of pss during several hours. An example is given on Figure 1.

Throughout the tropical band, vertical salinity differences greater than 0.1 pss are observed in each ocean, mainly between 0 and 15°N latitude for the Atlantic and Pacific Ocean, throughout the Bay of Bengal and around the Indian coast. These zones of high salinity differences coincide with the average position of the InterTropical Convergence Zone (ITCZ) and of Northern Indian Ocean Monsoon, so are likely to be related to precipitation (black boxes). Isolated large differences near coastlines and river mouths (e.g. the River Amazon along the Brazilian coast, the Congo and Niger along the African coast, and the Gulf of Mexico) are observed (red circles). Nevertheless, the mean of the salinity differences, calculated over the whole time period, either for each ocean or for each vertical level, remains less than 0.05 pss (0.027 pss over the whole dataset). The number of salinity

differences larger than 0.1 pss is less than 5% of the whole dataset. This percentage increases when the shallowest measurements is made at 1 m depth (7% for ΔS_{5-1} and more than 10% salinity differences higher than 0.1 pss for ΔS_{10-1}).

The locations of high 3d max rain rates coincide with locations of large vertical salinity differences, especially in the Atlantic Ocean (see Figure 2). When considering vertical salinity differences collocated with 3d max rain rate less than 10 mm hr^{-1} , only 5.3% of these salinity differences are larger

than 0.1 pss while when considering vertical salinity differences collocated with 3d max rain rate larger than 10 mm hr^{-1} , the percentage increases to 23.9%.

Salinity Working Group (2007), Argo salinity measurements shallower than 5 m are needed, and more series of measurements need to be obtained in the first meter of the ocean, particularly in the tropical ocean.

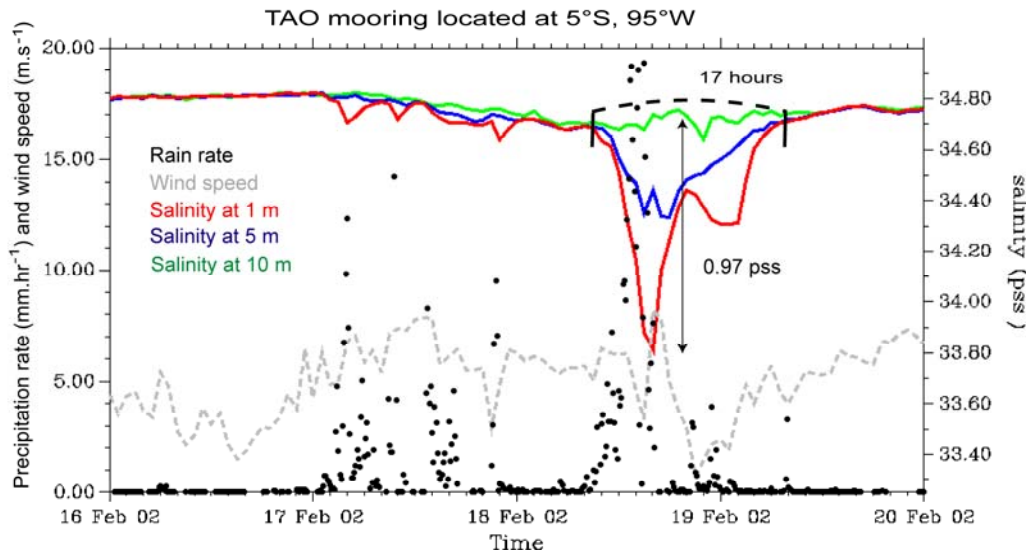


Figure 1: Influence of rainfall on salinity measurements at 1 m depth (red), at 5 m depth (blue) and 10 m depth (green) measured by a TAO mooring located at 5°S, 95°W. The black dots represent the rain rate measured every 10 minutes (mm.hr^{-1}) and the gray dotted line, the hourly mean wind speed (m.s^{-1}). The 18 Feb. 2002, the recorded precipitation is close to 23 mm/h .

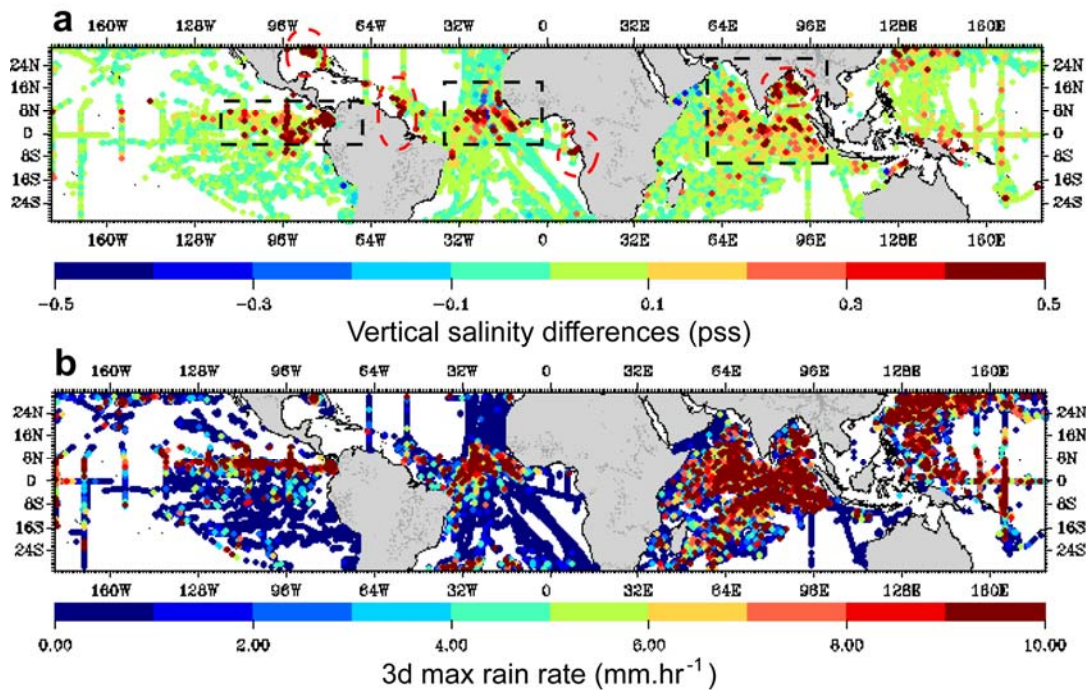


Figure 2: (a) Spatial distribution of vertical salinity differences. The colorbar indicates the value of salinity differences. (pss). (b) Spatial distribution of 3d max rain rate associated with vertical salinity differences. The colorbar indicates the value of 3d max rain rate (mm.hr^{-1}). In order to draw attention to the extremes, when several values of vertical salinity differences or 3d max rain rate occur at the same point, only the highest absolute values are displayed.

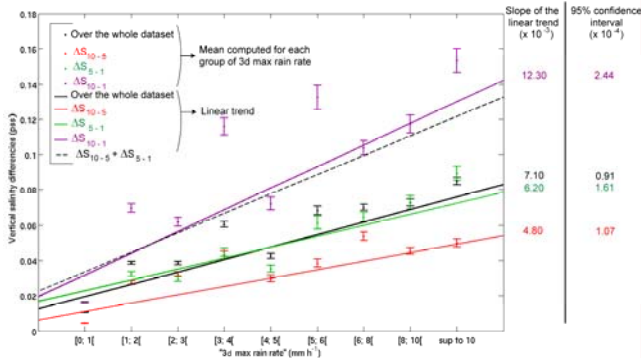


Figure 3: Vertical salinity differences versus 3d max rain rate for the different vertical levels (red for ΔS_{10-5} , green for ΔS_{5-1} , and purple for ΔS_{10-1}) and for the whole sorted dataset (black dots and curve). Errors bars represent the mean \pm 1 standard deviation. The black dotted curve represents the comparison between the linear trend associated with ΔS_{10-1} (purple curve) and the linear trend associated with $\Delta S_{10-5} + \Delta S_{5-1}$. The different slopes of linear trends and their associated 95% confidence intervals are indicated on the right hand side of the figure.

In order to examine if a relationship between vertical salinity differences and 3d max rain rate can be drawn, a linear regression is computed for the whole collocated dataset and for each vertical level (see Figure 3).

Statistically, the larger the 3d max rain rate is, the larger the vertical salinity difference is. In addition, the slope increases when 1 m SSS are considered, consistent with larger differences close to sea surface. The comparison of the slopes of the linear trends for the three vertical levels shows the validity of this statistical approach. Although more than 60 % of vertical salinity differences included in ΔS_{10-5} do not originate from the same vertical profiles as the salinity differences included in ΔS_{10-1} and ΔS_{5-1} , the sum of the linear trends of ΔS_{10-5} and ΔS_{5-1} is very close to the ΔS_{10-1} linear trend.

Discussion and Conclusion

Given that it will be necessary to average SMOS SSS over 10 days and 200 x 200 km² to reach an accuracy of 0.1-0.2 pss, we examine the vertical salinity differences averaged over 10 days on TAO/PIRATA moorings. On some moorings, salinity differences between 10 m and 1 m depth remain larger than 0.1 pss for more than one month (see Figure 4) reaching up to 0.5 pss. Even if the geographical extent of a rain event barely equals 200 x 200 km², mixing and ocean surface currents can spread fresh water, extending the impact of rainfall and creating artificial biases between SMOS and in situ salinity measurements.

Rain events can create a vertical salinity differences between SMOS and in situ SSS on the order of 0.1 – 0.2 pss at GODAE scale (200 km x 200 km and 10 days). The 3d max rain rate appears to be a reliable parameter for the detection of vertical salinity differences, via a statistical approach. Some recommendations can be drawn from this study to optimize SMOS calibration and validation phase: first, a detailed and complete check-up of in situ measurements has to be done to avoid suspicious or averaged data; then agreeing with the recommendations of the US CLIVAR

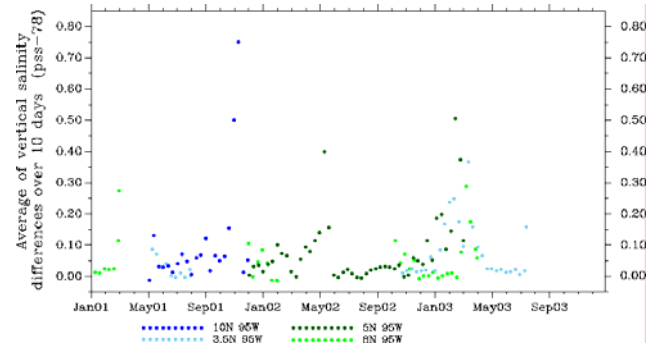


Figure 4: The average of vertical salinity differences between 10 m depth and 1 m depth over 10 days for 4 TAO moorings. Each color represents a different mooring, its location indicated on the right.

Acknowledgments

The authors are indebted to T. Delcroix, F. Gaillard and J. Gourrion for their scientific and technical advice and S. Le Reste and B. Bourles for their helpful explanations about the functioning of Argo floats. The authors wish to thank all the people participating in the Argo floats dissemination and the Argo technical and scientific team for providing free access to the Argo measurements. We also acknowledge G. Rohardt and all the Polarstern team for their help and for providing data, the SISMER team and the TAO Project Office of NOAA/PMEL, T. Boyer & the National Oceanographic Data Center, Remote Sensing Systems, and NASA Earth Science REASON DISCOVER Project for providing free and open access to, respectively, TAO and PIRATA data, the World Ocean database 2005, and measurements from SSM/I, TMI, and AMSR-E satellites. The authors are indebted to N. Martin for his computing support and valuable help

References

- Arnault, S., N. Chouaib, et al. (2004). "Comparison of Topex/Poseidon and Jason Altimetry with Aramis In Situ Observations in the Tropical Atlantic Ocean." *Marine Geodesy* 27:1: 15-30.
- Boyer, T. P., J. I. Antonov, et al. (2006). *World Ocean Database 2005*. S. Levitus, Ed., NOAA Atlas NESDIS 60, U.S. Government Printing Office, Washington, D.C.: 190 pp., DVDs.
- McPhaden, M. J. (1995). "The Tropical Atmosphere-Ocean array is completed." *Bulletin of the American Meteorological Society* 76.
- US_CLIVAR_Salinity_Working_Group (2007). Report of the U.S. CLIVAR Salinity Science Working Group. 2007-1: US CLIVAR Office, Washington, DC. Available online at http://www.usclivar.org/Pubs/Salinity_final_report.pdf.

Barrier Layer Variability in the Western Pacific Warm Pool, as inferred from Argo floats during 2000-2007

Christelle BOSC¹, Thierry DELCROIX¹ and Christophe MAES²
LEGOS, (UMR: CNES, CNRS, IRD, UPS); ¹Toulouse, ²Nouméa

Introduction

The Western Pacific Warm Pool (WP) is the warm source of the Earth's heat engine. It is characterized by permanent Sea Surface Temperature (SST) warmer than 28-29°C and Sea Surface Salinity (SSS) lower than 35 reflecting heavy precipitation (>3 m/year). Several past studies indicate that 'weak' oceanic and atmospheric changes in the WP are of major climatic importance both at global scale and for El Niño Southern Oscillation (ENSO) dynamics (Palmer and Mansfield, 1984; Picaut et al., 2001; Hoerling and Kumar, 2003). Of main interest in this regard is the existence of a SSS front located at its eastern edge, associated with specific salinity stratification in the isothermal upper layer.

The SSS front has important consequences on the physics and related biogeochemical features of the equatorial Pacific (see the reviews by Picaut et al., 2001, and Le Borgne et al., 2002). Still, the WP is characterized by the presence of Barrier Layer (BL) located in between the bottom of the density and temperature mixed layers (Lukas and Lindstrom, 1991). As evidenced in model simulation studies, BL acts: a) to maintain warm SST in the WP by isolating the density mixed layer from entrainment cooling at the bottom of the mixed layer, and b) to favor the WP displacements by confining the response to wind forcing in a shallower mixed layer (Maes et al., 1998; Vialard and Delecluse, 1998ab; Vialard et al., 2002).

There are rather few studies documenting the observed BL variability in the equatorial Pacific, chiefly because it requires long time series of concurrent temperature and salinity profiles with adequate vertical resolution. Taking advantage of Argo profiling floats (Roemmich and Owens, 2000), Bosc et al. (2007) have already demonstrated the potential of using such data to study the thermohaline variability in the WP. In line with their analysis, this study takes benefit from Argo data to analyze the conjoint relationships between the BL variability and the zonal SSS front, and focuses on the responsible mechanisms for BL formation during the period 2000-2007.

Data and data processing

Our study is based on a collection of temperature and salinity data collected in the equatorial Pacific (120°E-120°W, 5°N-5°S) during the period 2000-2007. Those data originate mainly from Argo floats (12 000 profiles, Figure 1) complemented by CTD profiles, and surface-only thermosalinograph (TSG) data. For Argo floats, only the so-called 'good data only' were downloaded from the Coriolis operational data centre, and we conducted additional tests to filter out spurious data over the 0-200 m depth range. For each Argo and CTD profile, the temperature and salinity values were then interpolated every 5 m using a spline function. Following de Boyer Montégut et al. (2004), the Isothermal and Mixed Layer Depths (ILD and MLD, respectively), and the resulting Barrier Layer Thickness (BLT) were then computed from each vertically-interpolated profile. Finally, values of SSS, SST, MLD, ILD, and BLT were

interpolated onto a regular grid of 5° in longitude, 1° in latitude and every 2 weeks, covering the 5°N-5°S, 120°E-120°W region during the period 2000-2007. Details can be found in Bosc (2008) and Bosc et al. (2008).

Surface structure variability

Figure 2 shows the longitude – time plot of 2°N-2°S averaged zonal surface salinity gradient ($\partial S/\partial x$), together with the longitudinal position of its maximum, and the Southern Oscillation Index (SOI). Values of $\partial S/\partial x$ reveal the well-marked contrast between the low-salinity waters of the western equatorial Pacific and the relatively high-salinity waters of the central equatorial Pacific. Statistical analyses based on correlation coefficients and ratios of zonal displacements indicate that it is the location of the 34.7 isohaline, as compared to other tested isohalines, which best agrees with the location of maximum $\partial S/\partial x$ denoting the SSS front ($R=0.87$). Figure 2 further reveals that the eastern edge of the WP was displaced eastward during El Niño years (2002, 2004, and 2006) and westward during La Niña years (2000-2001, 2007), out of phase with the SOI. Corroborating earlier results, we demonstrated that these displacements of the eastern edge of the WP were mainly induced by zonal current anomalies (not shown here, see Bosc et al., 2008).

Sub-surface structure variability

Figure 3 shows the longitude – time plot of 2°N-2°S averaged BLT, together with the area enclosed by SST warmer than 29.5°C and the position of the SSS front (as shown on Fig. 2). Interestingly, it indicates that the BL thicker than 15 m are only and permanently present (except for 2-3 months in 2001) in a zonal band extending from about 10° longitude to the east to 20° longitude to the west of the moving front position, whereas the BL thicker than 25 m mostly appear to the west of the front. A quantitative analysis shows that BLT within the 10 and 40 m range are almost linearly related to the strength of the zonal SSS gradient (not shown here). The maximum $\partial S/\partial x$ which is well suited to characterize the eastern edge of the warm pool, may be thus viewed as an additional source of information about the expected thickness of the BL, a feature which cannot be obtained in using any particular isohaline (such as the 34.7 for instance). As a consequence, we can expect that the combination of in situ and future satellite-derived SSS measurements (e.g., Kerr et al., 2001) will be quite useful, not only in locating the SSS front and derived BL location, but also in providing estimates of BLT in the western equatorial Pacific.

Figure 3 further reveals the outstanding time/space coincidence between the warmest (>29.5°C) SST and the thickest (>20 m) BL. Again, a quantitative analysis (not shown here) shows that 'hot' spots in SST (>29°C) can so barely occur without the presence of a thick (>20 m) BL, stressing the likely relevant climatic impact of thick BL (more in Bosc et al., 2008).

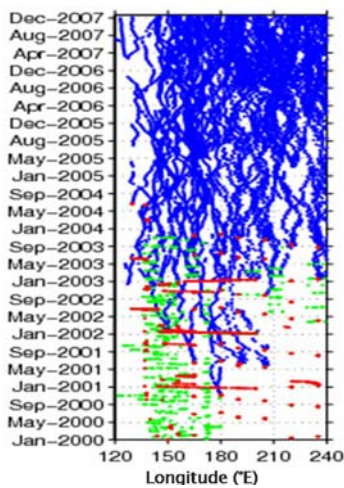


Figure 1. Longitude-time distribution of Argo floats (blue dots), CTD stations (red dots) and TSG (green dots) within 5°N-5°S.

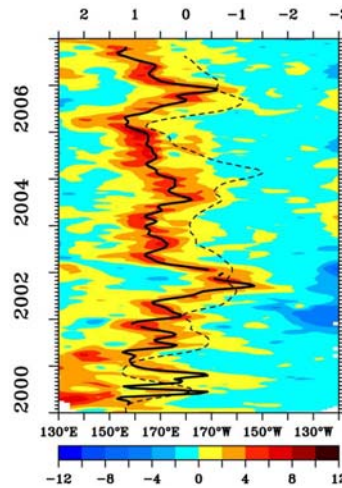


Figure 2. Longitude-time distribution of 2°N-2°S averaged zonal SSS gradient, $\partial S/\partial x$ (Units are $10^{-7} m^{-1}$). The heavy black line represents the maximum $\partial S/\partial x$. The dashed line denotes the Southern Oscillation Index scaled in reversed order on the upper horizontal axis.

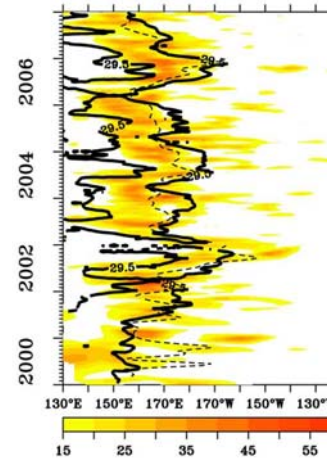


Figure 3. Longitude-time distribution of 2°N-2°S averaged barrier layer thickness (Units are m). The dashed black line represents the maximum $\partial S/\partial x$. The thick black lines denote the 29.5°C isotherm. Note that barrier layer thicknesses in excess of 15m only are reported.

Barrier layer formation mechanisms

Previous studies have revealed that the mechanisms responsible for changes in the BLT in the WP are rather complex and probably interrelated (e.g., Lukas and Lindstrom, 1991; Vialard and Delecluse, 1998ab). Local processes such as the effects of winds, precipitations and currents are detailed in Bosc et al. (2008) and, for this note, we will only focus on the role of equatorial waves for BL formation.

Previous studies have suggested that notable changes in BLT could result from equatorial waves acting remotely on the MLD and ILD (Shinoda and Lukas, 1995; Vialard and Delecluse, 1998b; Delcroix and McPhaden, 2002; Cronin and McPhaden, 2002). One possible explanation is that the amplitude of the vertical velocity associated with long equatorial waves increases downward in the upper ocean (Eriksen, 1982), meaning that the related vertical displacements are larger at the ILD than at the MLD, a feature that could favour a thickening of the BL (in case of downward velocity). To look at this possible process, Figure 4 shows the longitude-time plots of the 2°N-2°S averaged contribution of the first baroclinic Kelvin waves and first meridional mode ($m=1$) Rossby waves to the Sea Level Anomalies (SLA), as derived by Bosc and Delcroix (2008). Overplotted in Figure 4 are the anomalies of BLT relative to the same 2000-2007 period. It is interesting to note that there is clear tendency for downwelling (SLA>0) Kelvin and Rossby waves to coincide with the positive anomalous BLT. This happened, in particular, east of about 170°E during the 2nd half of 2002, 2004 and 2006 for downwelling Kelvin waves, and about every year for the westward propagating downwelling Rossby waves. Hence, the BL appears to be thicker-than-average in the presence of downwelling Kelvin and Rossby waves, and thinner-than-average for upwelling waves.

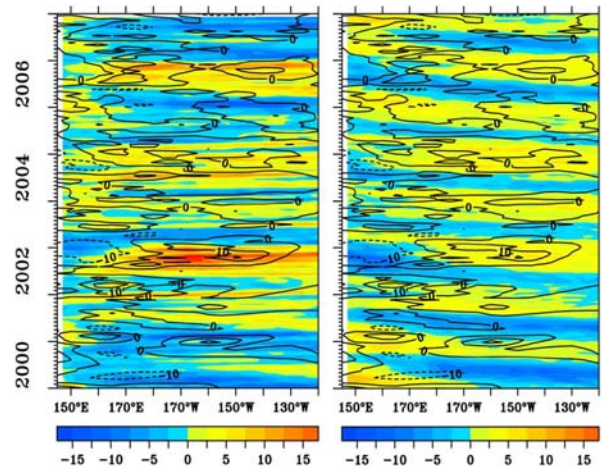


Figure 4. Longitude-time distribution of 2°N-2°S averaged sea level anomalies (cm) associated with first baroclinic Kelvin (left panel) and first meridional mode Rossby (right panel) waves. Positive values denote downwelling equatorial waves. The black contours on both panels show the 2°N-2°S averaged barrier layer thickness anomalies (m). All anomalies are relative to the 2000-2007 period.

REFERENCES

- Bosc, C., Variabilité du volume d'eau chaude et de la couche barrière de sel dans l'océan Pacifique équatorial à l'échelle interannuelle (ENSO), *Doctorat de l'Université P. Sabatier, Toulouse, France*, 158 pp, 2008.
- Bosc C., C. Maes and T. Delcroix, Thermohaline Variability of the Eastern Edge of the Western Pacific Warm Pool, as inferred from ARGO floats, *Coriolis newsletter n°4*, sept 2007.
- Bosc, C., T. Delcroix and C. Maes, Barrier Layer Variability in the Western Pacific Warm Pool During the period 2000-2007, *J. Geophys. Res.*, submitted, 2008.
- Bosc, C., and T. Delcroix, Observed equatorial Rossby waves and ENSO-related warm water volume changes in the equatorial Pacific Ocean. *J. Geophys. Res.*, 113, C06003, doi:10.1029/2007JC004613, 2008.
- Cronin, M. F., and M. J. McPhaden, Barrier layer formation during westerly wind bursts, *J. Geophys. Res.*, 107(C12), 8020, doi:10.1029/2001JC001171, 2002.
- de Boyer Montégut, C., G. Madec, A. S. Fischer, A. Lazar, and D. Ludicone, Mixed layer depth over the global ocean: An examination of profile data and a profile-based climatology, *J. Geophys. Res.*, 109, C12003, doi:10.1029/2004JC002378, 2004.
- Delcroix, T., and M. J. McPhaden, Interannual sea surface salinity and temperature changes in the western Pacific warm pool during 1992–2000, *J. Geophys. Res.*, 107(C12), 8002, doi:10.1029/2001JC000862, 2002.
- Eriksen, C., Equatorial wave vertical modes observed in a western Pacific Island Array, *J. Phys. Oceanogr.*, 12, 1206-1227, 1982.
- Hoerling, M., and A. Kumar, The perfect ocean for drought, *Science*, 299(5607), 691-694, 2003Kerr, Y., .P. Waldteufel, J.P. Wigneron, J.M. Martinuzzi, J. Font, and M. Berger, Soil moisture retrieval from space: The Soil Moisture and Ocean Salinity (SMOS) mission. *IEEE Transactions on Geoscience and remote sensing*, 39(8), 1729-1735, 2001.
- Le Borgne, R., R. Barber, T. Delcroix, H. Inoue, D. Mackey, and M. Rodier, Pacific warm pool and divergence : temporal and zonal variations on the equator and their effects on the biological pump, *Deep Sea Res.*, 49, 2471-2512, 2002.
- Lukas, R., and E. Lindstrom, The mixed layer of the western equatorial Pacific Ocean, *J. Geophys. Res.*, 96, suppl., 3343–3357, 1991.
- Maes, C., P. Delecluse, and G. Madec, Impact of westerly wind bursts on the warm pool of the TOGA-COARE domain in an OGCM, *Clim. Dyn.*, 14, 55–70, 1998.
- Palmer, T. N., and D.A. Mansfield, Response of two atmospheric general circulation models to sea-surface temperature anomalies in the tropical east and west Pacific, *Nature* 310, pp. 483–488, 1984.
- Picaut, J., M. Ioualalen, T. Delcroix, F. Masia, R. Murtugudde, and J. Vialard, The oceanic zone of convergence on the eastern edge of the Pacific warm pool: A synthesis of results and implications for ENSO and biogeochemical phenomena, *J. Geophys. Res.*, 106, 2363– 2386, 2001.
- Roemmich, D., and W. B. Owens, The Argo Project: Global ocean observations for understanding and prediction of climate variability. *Oceanogr.*, 13, No. 2 (NOPP Special Issue), 45-50, 2000.
- Shinoda, T., and R. Lukas, Lagrangian mixed layer modelling of the western equatorial Pacific. *J. Geophys. Res.*, 100, 2523–2541, 1995.
- Vialard, J. and P. Delecluse, An OGCM Study for the TOGA Decade. Part I : Role of Salinity in the Physics of the Western Pacific Fresh Pool. *J. Phys. Oceanogr.*, 28, 1071 – 1088, 1998a.
- Vialard, J. and P. Delecluse, An OGCM Study for the TOGA Decade. Part II : Barrier Layer Formation and Variability. *J. Phys. Oceanogr.*, 28, 1089 – 1106, 1998b.
- Vialard, J., P. Delecluse, and C. Menkes, A modeling study of salinity variability and its effects in the tropical Pacific Ocean during the 1993–1999 period, *J. Geophys. Res.*, 107(C12), 8005, doi:10.1029/2000JC000758, 2002.

Next Meetings

- **10th Argo Steering Team Meeting**, Hangzhou, China, March 22-23, 2009.
- **3rd Argo Science Workshop**, Hangzhou, China, March 25-27, 2009.
- **2nd Euro-Argo User Workshop**, Trieste, Italy, June 16-19, 2009.
- **OceanObs09**, Venice, Italy, Sept. 21-25, 2009.
- **10th Argo Data Management Meeting**, Toulouse, France, Nov. 2009.

We would be interested in reading about the results of your work in a future Coriolis News Letter.
We welcome your contributions!



Editorial Board: Sylvie Pouliquen
Secretary: Francine Loubrieu
Contact: codac@ifremer.fr